

DETC97/VIB-4229

FATIGUE LIFE PREDICTIONS BY COUPLING FINITE ELEMENT AND MULTIBODY SYSTEMS CALCULATIONS

Stefan Dietz

Institute for Robotics and System Dynamics
German Aerospace Research Establishment (DLR)
82234 Wessling, Germany
& Aerospace Institute
Technical University of Berlin
Marchstr.12, 10587 Berlin, Germany
Email: dietz@ice.fb12.tu-berlin.de

Helmuth Netter, Delf Sachau

Institute for Robotics and System Dynamics
German Aerospace Research Establishment (DLR)
82234 Wessling, Germany
Email: Helmuth.Netter@dlr.de, Delf.Sachau@dlr.de

ABSTRACT

The dynamic loads and accelerations acting on a railway bogie are predicted by multibody simulation. The bogie frame is considered as an elastic body of the MBS-model, in which elastic displacements are represented by eigen and static modes. Stresses are calculated for the most stressed locations of a bogie in the MBS-postprocessor. Based on these a fatigue life prediction is carried out.

NOMENCLATURE

M FE mass matrix
 K FE stiffness matrix
 p FE load vector
 Φ modal matrix
 q modal coordinates
 u displacement vector
 ϵ strain vector
 σ stress vector
 $M(q)$ MBS mass matrix
 $K(q)$ MBS stiffness matrix
 k MBS vector of gyroscopic forces
 h MBS vector of applied forces
 y MBS output vector
 a acceleration
 ω angular velocity
 A orientation matrix
 P covariance matrix

B stress-load matrix
 f force vector
 R Markov matrix
 ρ correlation coefficient
 D damage value
 x, y, z cartesian coordinates
 t time

1 INTRODUCTION

Due to the tendency towards lightweight structures, the elastic deformations of the components can no longer be neglected. Small deformations can be taken into consideration by using the preprocessor FEMBS in combination with the multibody simulation program SIMPACK, see figure 1 (Rulka and Eichberger, 1993).

The finite element method (FEM) is a valuable tool for vibration and stress analysis of structural parts and complete mechanical systems. A weakness of the approach lies in the assumptions made on the boundary conditions. Reliable information is generally available for static situations, but many mechanical systems are loaded dynamically. In such cases the determination of time varying boundary and load conditions can be determined by multibody simulation.

MBS-simulation delivers realistic loads for the analysis of strength of materials and life cycles calculations, because the dynamical behaviour of the vehicle, the excitation by the track, the vehicle velocity and other data, defining op-

erational conditions influence these loads. Two kinds of operational conditions are considered in order to obtain realistic results.

- The ride on a straight track causes small dynamic loads and movements, therefore the force laws and the wheel-rail-contact of the MBS-model can be assumed as linearized relations. In this case the MBS-calculation can be treated as a covariance analysis, by which the whole operational condition is simulated in one solution step. As MBS input data, the spectral densities of the *track irregularities* are required. Loads acting on the bogie are obtained as covariance matrix.
- In contrast to the operational condition mentioned above, crossing a switch for example produces large dynamic loads. For such *single irregularities* the force laws and the wheel-rail-contact are nonlinear. The MBS calculation is performed as a time integration and results in forces and accelerations for each time step.

An important task is the identification of the most stressed or critical locations. For that, the loads and accelerations for some time steps can be transformed into a FE-load vector by the MBS-postprocessor $FEMBS^{-1}$. Subsequently a FEM calculation is performed and the visualisation of the stresses shows the critical locations.

The distinction between linear and nonlinear operational conditions is useful to avoid large MBS-simulation times, because there is no need for simulations over distances, which are several miles long. MBS-simulations are performed for all operational conditions separately. Information about the length of the straight track, the number of switches and the frequency of other possible situations are given subsequently, inside the MBS-postprocessor FATIGUE. In FATIGUE the magnitude of damage for the critical locations is determined for all operational conditions separately and they can be superimposed to the total damage value in a last step. Because the calculation of damage values from the MBS-results takes only a few minutes, the investigation of a multitude of situations is feasible.

2 FE-MBS COUPLING

Flexible Bodies in Multibody Systems

The coordinate systems shown in figure 2 will be used to describe the body's motion. They are the inertial frame and the body fixed reference frame. In general all vectors will be resolved in the reference frame. The motion of a representative material point P with respect to inertial space is described as

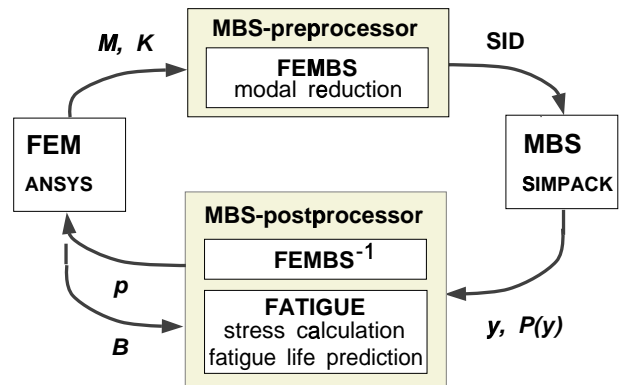


Figure 1. FE-MBS coupling scheme

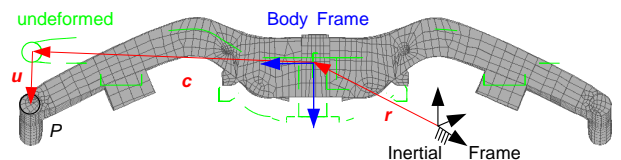


Figure 2. Flexible body; 3rd eigenmode: vertical bending at 52 Hz

$$r^P = r(t) + c + u(c, t). \quad (1)$$

In this representation the body motion is given in terms of the reference or rigid body motion as described by $r(t)$ and c and in terms of small displacements $u(c, t)$. A Ritz-approximation of the deformation variables

$$u(c, t) = \Phi(c)q(t) \quad (2)$$

is used with the unknown modal coordinates $q(t)$. Here eigen and static modes calculated by the finite element code ANSYS are used as interpolation functions $\Phi(c)$

$$\Phi = [\Phi_{eig}, \Phi_{stat}]. \quad (3)$$

The starting point for the development of the $O(N)$ -formalism in SIMPACK is a set of equations of motion for the flexible bodies. Introducing the Ritz-approximation into Hamilton's principle and using the fundamental theorem of

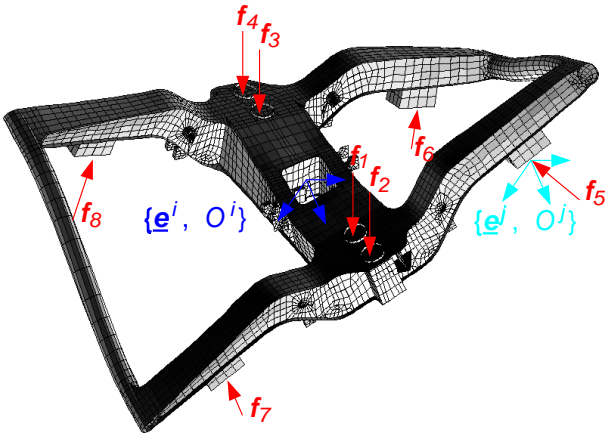


Figure 3. Dynamically loaded elastic body; f_1 to f_4 secondary suspension forces f_5 to f_8 primary suspension forces; 1st eigenmode: torsion at 42 Hz

variational calculus the equations of motion result as follows

$$\mathbf{M}(\mathbf{q}) \begin{Bmatrix} \mathbf{a} \\ \dot{\boldsymbol{\omega}} \\ \ddot{\mathbf{q}} \end{Bmatrix} + \mathbf{k}(\boldsymbol{\omega}, \mathbf{q}, \dot{\mathbf{q}}) + \begin{Bmatrix} \mathbf{0} \\ \mathbf{0} \\ \mathbf{K}(\mathbf{q})\mathbf{q} \end{Bmatrix} = \mathbf{h}(\mathbf{r}, \mathbf{A}, \mathbf{q}, \dots); \quad (4)$$

Matrix \mathbf{M} contains inertia terms, \mathbf{k} gyroscopic terms, \mathbf{K} stiffness terms and \mathbf{h} the applied forces. The flexible body data required to generate the MBS-equations are those, which are needed to compute the elements of the mass matrix, the gyroscopic terms and the stiffness terms. To compute such data the preprocessor FEMBS has been developed, (Wallrapp and Sachau, 1994). The data are stored in the standard-input-data (SID) file, (Wallrapp, 1994). The relative orientation matrix $\mathbf{A}_{ij}(\mathbf{q})$ is developed up to linear terms in the displacement coordinates, (Wallrapp and Sachau, 1994). While reading the SID file SIMPACK automatically assigns the MBS-marker to the corresponding FE-nodes.

Possibilities for stress calculation

MBS-Postprocessor FEMBS⁻¹ The time history of all forces and torques acting on the flexible body are calculated during the MBS simulation. In the postprocessor FEMBS⁻¹ the markers on the body are checked and the forces resulting from joints, force laws or constraints at each marker are collected and transformed in the body coordinate system $\{e^i, O^i\}$ at each time step, (Braun, 1995). The postprocessor FEMBS⁻¹ generates files to be used in:

- **ANSYS:** Some time steps are selected by the user for which the FEM load vector is generated ready to

be used in quasistatic finite element calculations. The FEM-calculation delivers the stress distribution for the whole body under consideration. From these results critical locations with maximal stresses in the body can be found.

- **FATIGUE:** The time histories of loads as calculated by the MBS-code are written to a file, to be used for life prediction. The MBS-loads are transformed into stresses at some critical locations.

For linear systems the covariance matrix of the forces can be calculated directly by SIMPACK.

MBS-Postprocessor FATIGUE Because of the large number of degrees of freedom, approximately 100000 for a bogie frame, stress calculations in the FE-code are not practicable within each time step. Another method is implemented in FATIGUE, which takes advantage of the linear FE-model. Loads and accelerations, acting on the bogie, can be defined in SIMPACK as MBS output vector \mathbf{y} and the stresses $\boldsymbol{\sigma}$ depends on them, via the stress load matrix \mathbf{B}

$$\underbrace{\begin{Bmatrix} \sigma_x \\ \sigma_x \\ \sigma_x \\ \tau_{xy} \\ \tau_{yz} \\ \tau_{xz} \end{Bmatrix}}_{\boldsymbol{\sigma}(\mathbf{c}, t)} = \underbrace{\begin{bmatrix} \sigma_x(a_x = 1) \dots \sigma_x(f_x = 1) \dots \\ \sigma_x(a_x = 1) \dots \sigma_x(f_x = 1) \dots \\ \sigma_x(a_x = 1) \dots \sigma_x(f_x = 1) \dots \\ \tau_{xy}(a_x = 1) \dots \tau_{xy}(f_x = 1) \dots \\ \tau_{yz}(a_x = 1) \dots \tau_{yz}(f_x = 1) \dots \\ \tau_{xz}(a_x = 1) \dots \tau_{xz}(f_x = 1) \dots \end{bmatrix}}_{\mathbf{B}(\mathbf{c})} \underbrace{\begin{Bmatrix} a_x(t) \\ \vdots \\ f_x(t) \\ \vdots \end{Bmatrix}}_{\mathbf{y}(t)}. \quad (5)$$

The stress load matrix is calculated for those locations, for which the FEMBS⁻¹-ANSYS postprocessing indicates high stresses. It contains column by column pre-calculated stresses for unit loads, unit accelerations and eigenmodes. The elements of the MBS-output vector are time dependent weighting factors for them. In (Dietz and Knothe, 1997) a way for pre-calculating stresses is described.

For linear operational conditions the MBS-output is given by the covariance matrix

$$\mathbf{P}(\mathbf{y}) = \lim_{T \rightarrow \infty} \int_0^T \mathbf{y} \mathbf{y}^T dt \quad (6)$$

and the time independent stress load matrix allows the transformation of $\mathbf{P}(\mathbf{y})$ into a stress covariance matrix

$$\mathbf{P}(\boldsymbol{\sigma}) = \mathbf{B} \mathbf{P}(\mathbf{y}) \mathbf{B}^T. \quad (7)$$

3 FATIGUE LIFE PREDICTION

Lots of information about the stresses have to be reduced, because we are only interested in the most stressed locations of the bogie frame and the magnitude of damage for these locations. For it, a procedure proposed by (Stichel, 1996) is used in FATIGUE.

Stress evaluation in the time domain

For the whole time history of stress the range between the maximum and the minimum values of stresses is divided into equidistant intervals, or classes n_σ , see figure 4 a. Considering a nonlinear stress strain relationship $\epsilon = f(\sigma)$, the classified time history of stress can be mapped into the stress strain plane. Figure 4 b shows 3 closed stress strain hysteresis loops, which are mainly responsible for the fatigue of the material and therefore counted by the rainflow method. The total number of hysteresis loops or cycles n_c , the start of the cycle n_{σ_1} and its reversal point n_{σ_2} , is stored in a Markov matrix \mathbf{R} , in which each element $(r_{n_{\sigma_1}, n_{\sigma_2}})$ equals to n_c , see figure 5 a. For harmonic processes it is known, that the stress amplitude limit $\lim \sigma_a$ is decreasingly for increasing steady state stress σ_m . The gradient Ψ of this linear relationship can be calculated for instance from Smith fatigue strength diagram, shown in figure 5 b. Assuming this relationship also for stochastic processes, Ψ depends on the material and the stress evaluation method. For stochastic loaded steel constructions and the rainflow stress evaluation, a Ψ -value of 0.3 is recommended in (Stichel, 1996). The present stress amplitude σ_a and the steady state stress can be calculated from the Markov matrix by equation (8) and (9). Each cycle of the process stored in the Markov matrix will be transformed by equation (10) into a cycle, in which the steady state stress is zero and the stress amplitude is magnified

$$\sigma_m = (\sigma_2 + \sigma_1)/2.0, \quad (8)$$

$$\sigma_a = (\sigma_2 - \sigma_1)/2.0, \quad (9)$$

$$\sigma_{ae} = \sigma_a + \Psi \sigma_m. \quad (10)$$

By the magnification of stress amplitudes the damaging effect of the steady state stress components is taken into account. Cumulative frequency distributions, describing an equivalent stochastic process without steady state stresses are the result of the transformation given by equation (10).

Stress evaluation in the frequency domain

Although the stress covariance matrix contains the mean square values of the stresses, it is possible to calculate the number of stress cycles. Therefore a probability

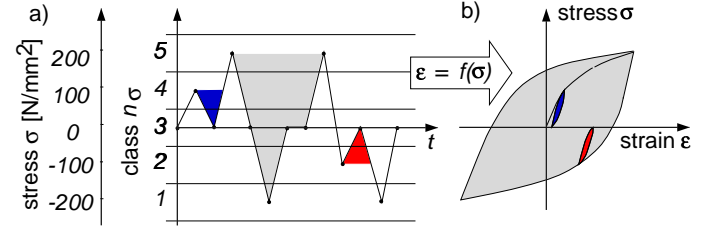


Figure 4. Stress evaluation with the rainflow method: Time history of stress a) divided into 5 classes n_σ ; time history mapped into the stress strain plane b) with 3 closed hysteresis loops counted by rainflow method

distribution function describing the random process is assumed, whereby its parameters can be calculated from the stress covariance matrix, see below. The Rayleigh distribution $f_R(\sigma_a)$ and the Gaussian distribution $f_G(\sigma_m)$ were combined multiplicatively by Kowalewski and Sjöström to describe the distribution of the steady state stresses and the stress amplitudes. The integration of this distribution $f_R f_G$ yields the number of cycles

$$nc = N_1 \int \int \underbrace{\frac{\sigma_a}{s_0^2 i^2} e^{\left(\frac{-\sigma_a^2}{2s_0^2 i^2}\right)}}_{f_R} \underbrace{\frac{1}{\sqrt{2\pi s_0 \nu}} e^{\left(\frac{-\sigma_m^2}{2s_0^2 \nu^2}\right)}}_{f_G} d\sigma_a d\sigma_m. \quad (11)$$

Therefore the steady stress and amplitude stress range is divided into classes n_{σ_m} and n_{σ_a} again. In figure 6 the integration is taken over the dark grey area. This yields the number of cycles n_c for the class $n_{\sigma_a} = 2$ and $n_{\sigma_m} = 9$. The integration for each class results in a matrix, in which the number of cycles is stored for each class. This matrix also can be mapped to a cumulative frequency distribution by equation (10), where ψ is set to 0.7 (Stichel, 1996). The parameters of equation (11) will be derived subsequently from the statistical characteristic values

$$s_{2j}^2 = \lim_{T \rightarrow \infty} \frac{1}{T} \int_{t=0}^T \left[\left(\frac{\partial}{\partial t} \right)^j \sigma(t) \right]^2 dt. \quad (12)$$

If the first and second derivatives of the forces are included in the MBS-output vector s_0, s_2 and s_4 can be taken from the main diagonal of the stress covariance matrix.

$$N_0 = s_2 / (2\pi s_0), \quad (13)$$

$$N_1 = s_4 / (2\pi s_2), \quad (14)$$

$$i = N_0 / N_1, \quad (15)$$

$$\nu = \sqrt{1 - i^2}. \quad (16)$$

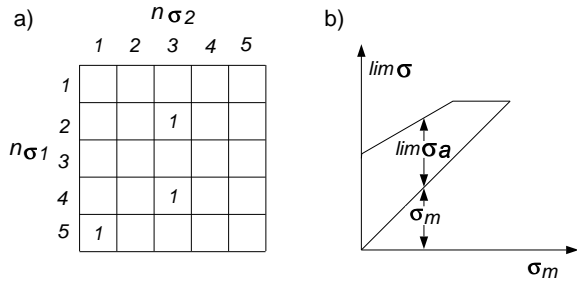


Figure 5. Calculating the data for amplitude transformation, see equation (8) to (10): From the Markov matrix a), which results from the process shown in figure 4 and from Smith fatigue strength diagram b)

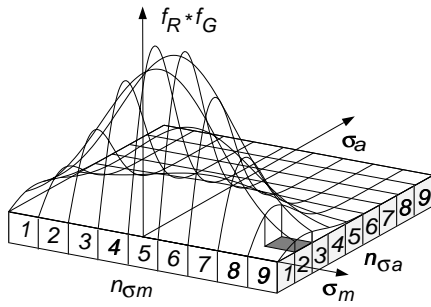


Figure 6. Probability distribution for the steady state stresses and the stress amplitudes

The frequency of stress peaks N_1 and increasing zero passages N_0 results in the irregularity value i and the width of the frequency band ν , which are parameters of the distribution functions for f_R and f_G .

Calculation of damage values

The calculations described above, are performed for all critical locations of the bogie frame and all components of the stress tensor. The rainflow method as well as the Kowalewski method combined with the amplitude transformation (10) are resulting in cumulative frequency distributions. As the FE-Model of the bogie frame consists of shell elements, only the cumulative frequency distributions of the normal stresses σ_x and σ_y and the shear stress τ_{xy} are considered subsequently. In usual fatigue strength-diagrams, see figure 5 b), the stress limit $lim\sigma$ is derived from fatigue tests, which are based on harmonic processes. Therefore all these distributions will be mapped to an equivalent harmonic process which causes the same damage to the critical locations as the equivalent stochastic process, see figure 7

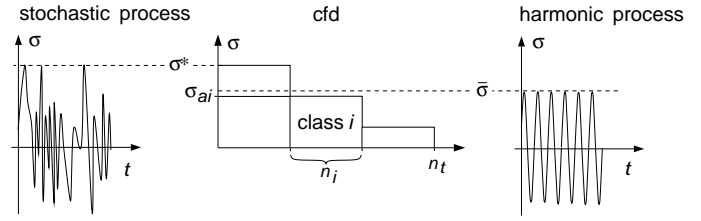


Figure 7. Mapping the equivalent stochastic process to an equivalent harmonic process using cumulative frequency distributions (cfd)

and equation (17).

$$\bar{\sigma}_x = \frac{1}{\left(\underbrace{\sum_i \frac{n_i}{n_t} \left(\frac{\sigma_{xai}}{\sigma_x^*} \right)^6}_{\nu} \right)^{-0.787} \left(\frac{2.0 \cdot 10^6}{n_t} \right)^{1/6.5}} \sigma_x^* \quad (17)$$

From the shape ν of the cumulative frequency distribution and the duration n of the operational condition, a factor $1/\nu n$ reducing σ^* to $\bar{\sigma}$ is calculated. The stress limit $lim\sigma$ can be taken from a usual fatigue strength-diagram, where $lim\sigma$ is given as a function of the stress amplitude $\bar{\sigma}$ and the static stress $stat\sigma$. The present stresses and the stress limits are known yet, so the damage values can be calculated. In FATIGUE, damage values for the normal stress

$$D_{\sigma_x} = \frac{stat\sigma_x + \bar{\sigma}}{lim\sigma_x} \quad (18)$$

and the other elements of the stress tensor are calculated separately. At weldings for example, where the stress limit depends on the direction of stresses, this procedure is useful. The damage value D_{σ_x} is a measure for the magnitude of damage, resulting from the normal stress σ_x . Information about the correlation of σ_x and σ_y for instance, is given by the correlation coefficient $\varrho_{x,y}$

$$\varrho_{x,y} = \frac{\lim_{T \rightarrow \infty} \int_{t=0}^T \sigma_x \sigma_y dt}{\sqrt{\lim_{T \rightarrow \infty} \int_{t=0}^T \sigma_x^2 dt \lim_{T \rightarrow \infty} \int_{t=0}^T \sigma_y^2 dt}} \quad (19)$$

Those $\varrho_{i,j}$ can be interpreted as average phase angles between the elements of the stress tensor and they are required to meet the equilibrium of the stress components. For a single location of the bogie the damage value

$$D^2 = (\varrho_{x,x} D_{\sigma_x})^2 + (\varrho_{x,y} D_{\sigma_y})^2 + (\varrho_{x,x} D_{\sigma_x})(\varrho_{x,y} D_{\sigma_y})$$

$$+ (\varrho_{x,xy} D_{\tau_{xy}})^2, \quad (20)$$

is derived from the maximum shear strain criterion (Stichel, 1996).

4 LIFETIME CALCULATIONS FOR DIFFERENT OPERATIONAL CONDITIONS

FE-Model of the bogie frame

The welded bogie frame of the freight locomotive is approximately 5.5 m long and 2.4 m wide, its mass is about 2200 kg. The corresponding finite element model (ANSYS) consists of 9200 finite shell elements, see figure 3. Constraint equations are used, to distribute the external forces which act on the bogie. The FE model has approximately 50000 degrees of freedom. To ensure a realistic dynamical model, the first three eigenmodes of the unrestrained bogie are considered to setup the equations of motion for the multibody (SIMPACK) simulation (Wallrapp and Sachau, 1994). These are the torsion with a frequency of 42 Hz, see figure 3, vertical bending with a frequency of about 52 Hz, see figure 2 and lateral bending with a frequency of 48 Hz.

MBS-Model complete wheel-rail system

The freight locomotive model has been modelled with the aid of SIMPACK library elements like force elements and joints. The bogie frames were described as elastic bodies using the data from the SID-file as described above. Several linear spring and damper elements describe the primary and secondary suspension units. Nonlinear characteristics represent the bump stops or viscous dampers. Finally the multibody model of the freight locomotive consists of nine rigid bodies (carbody, four wheelsets and four driving motors) and the two elastic bodies or the bogie frames, see figure 8.

The two basic features of the railway functionality in SIMPACK are both, the description of the track to simulate arbitrary manoeuvres and the modelling of the contact between the interface of wheel and rail, (Stribersky et al., 1997), respectively. Common measured track data like curvature and superelevation can be used to obtain all necessary track quantities. A special track joint positions each wheel or wheelset along the track at arc-length $s(t)$ and also guarantees the simulation of acceleration and braking manoeuvres in curves. The general wheel-rail contact element models the normal contact of the wheel-rail interaction as kinematical constraint of the relative vertical displacement of the wheel with respect to the rail. Multiple contacts are allowed.

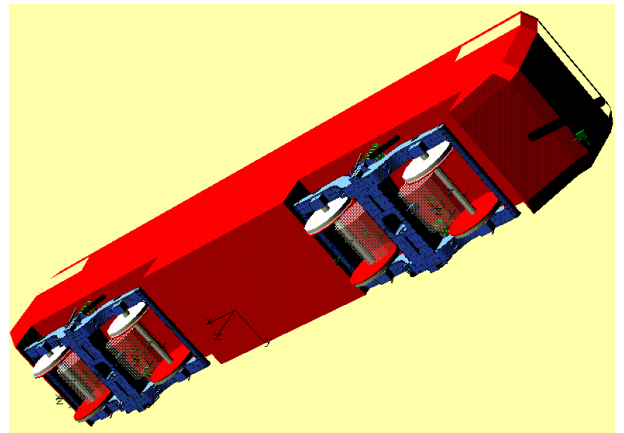


Figure 8. MBS-model of the freight locomotive

To investigate wheel lifts or impacts caused by short contact separations, the normal wheel-rail contact can also be modelled by a one-sided spring-damper element accepting increased CPU-simulation time compared to the constrained formulation because of a high value of contact stiffness. The calculation of the creep forces is based on Hertzian contact properties and uses Kalkers code FAST-SIM (1983) or any other creep law defined by the user. The elasticity of the track is taken into account by a rigid sleeper below each wheelset with three degrees of freedom with respect to the track interconnection to inertial system by linear spring and damper elements.

As a total the complete wheel-rail system model includes 64 joint states with 8 of these states restricted by constraints, 6 states describing the elastic deformation, 4 states describing dynamical force elements and 8 algebraic states representing the constraint forces of the constrained wheel-rail contacts.

Running through a switch

Figure 9 shows a top view of the switch with its major track and divergent route. On the right selected cross sections show the s -variable rail profiles of the common crossing and the check rail. The desired switch is about 40 m long, the diverging route describes a radius of 500 m.

In order to model the contact between back of wheel and check rail an additional wheel-rail element was introduced with elastic characteristic of the normal contact.

Simulation results The vehicle runs into the switch with constant velocity $V = 55 \text{ km/h}$ taking the divergent route. As it can be seen from figure 10 the leading wheelsets are shifted towards the outer rail with distinctive flange con-

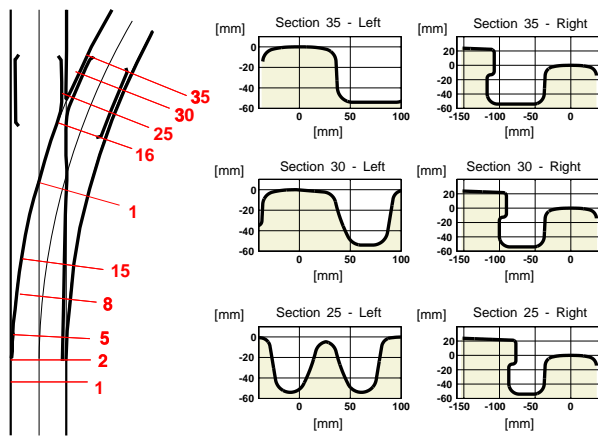
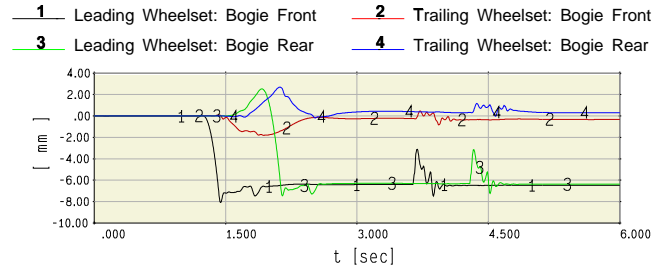


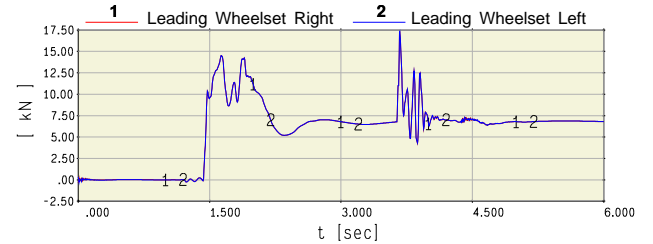
Figure 9. Geometry of the switch and selected cross sections

tact on the high wheels whereby the trailing wheelsets are retaining their center position. The influence of the varying rail profile geometry on the dynamics can be observed clearly looking at the forces acting in the primary suspension of the foremost wheelset. At time $t_1 = 1.63$ sec the wheelset passes the switch blade with double contact on the left wheel. The second oscillations are arising when the wheelset goes through the common crossing on left wheel and gets into hard contact between back of right wheel and the check rail at $t_2 = 3.67$ sec. After the multibody simulation has been performed, the time events where maximal forces act onto the bogie are considered. Here for the two time steps $t_1 = 1.63$ sec and $t_2 = 3.67$ sec all forces and the absolute motion of the bogie reference frame are transferred back to ANSYS using the FEMBS⁻¹ code. The quasistatic FE calculation for the time t_2 results in the stress distribution as shown in 11. From this figure locations of maximal stress can be identified. These locations are used later for fatigue life calculations. In figure 11 the most stressed locations 1 and 2 are marked and the accompanying time histories of stress $\sigma_x^1(t)$ and $\sigma_x^2(t)$ are shown in figure 12. The $\sigma_x^1(t)$ plot is correlated to the vertical primary forces, which are responsible for the vertical bending of the bogie. Location 2 marked in figure 12 is mainly sensitive against lateral bending, caused by lateral primary forces. Damage values for both locations are listed in table 2. Because the stresses from dynamic loads are small compared to the stresses from static loads (approximately 7%), the fatigue life calculation results in small damage values. Figure 12 shows a quite small number of stress cycles and in combination with the assumption, that a switch every 10 km occurs, small damage values are plausible, though the lateral dynamical forces are comparatively large, see table 1.

Lateral Deviation of Wheelsets



Primary Suspension Bogie Front: Lateral Forces



Primary Suspension Bogie Front: Vertical Forces

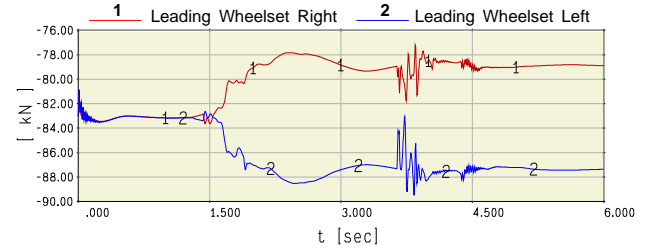


Figure 10. MBS-simulation results from SIMPACK : Freight locomotive crossing a switch; $V=55$ km/h; track gauge= 1435 mm; $1:\infty$; FASTSIM; $\mu = 0.4$; $R = 500$ m; switch : EW-UIC60-500-1:12-ZV

Riding on straight track

In order to apply linear system analysis a method based on harmonic balance is used for the quasi-linearization of the nonlinear wheel-rail-contact kinematics. The freight locomotive rides with its reference velocity of 140 km/h on the straight track, so this value is assumed to perform the covariance analysis. The track excitation is defined by standard power spectral density functions for the vertical, lateral and cross level track irregularities, see figure 13. As MBS-output quantities \mathbf{y} the vertical forces of the primary and secondary suspension are defined. From the covariance matrix $\mathbf{P}(\mathbf{y})$ RMS values were calculated and listed in table 1. The RMS values are a little smaller compared to the dynamically primary suspension forces, caused by passing

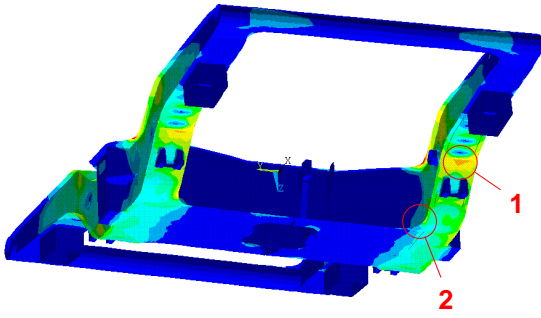


Figure 11. MBS-postprocessing with FEMBS¹ and ANSYS: Stress distribution for the whole bogie frame at $t_2 = 3.67$ sec; Locations marked as 1 and 2 were investigated with FATIGUE

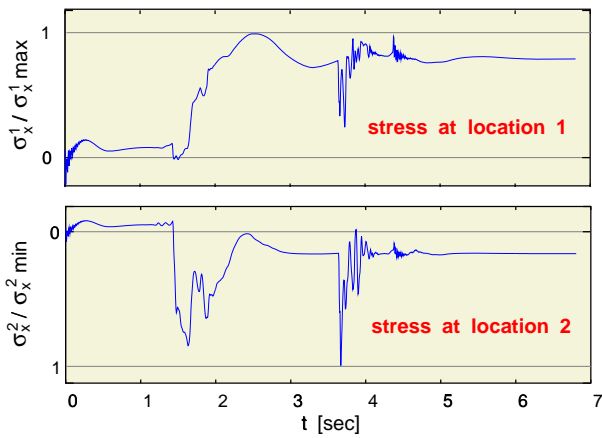


Figure 12. MBS-postprocessing with FATIGUE: Time histories for the normalized stresses $\sigma_x^{1,2}$ at the locations 1, 2, see figure 11

the switch, see figure 10. In opposite to that the damage values calculated from the straight track ride are greater than those, which were calculated from the switch ride, see table 2. This is why vibrations from the straight track ride are present permanently, whereas the switch ride occurs less frequently.

5 CONCLUSIONS

The dynamic loads acting on a railway bogie frame were calculated from a MBS-model of a freight locomotive, whereby the bogie frames are modeled as elastic bodies. By the MBS-postprocessor FEMBS⁻¹ these loads were transferred back to the FE-code, in which the stress distribution for the whole bogie was calculated and high stressed locations were indicated. The stress load matrix for two of those locations were used within the MBS-postprocessor

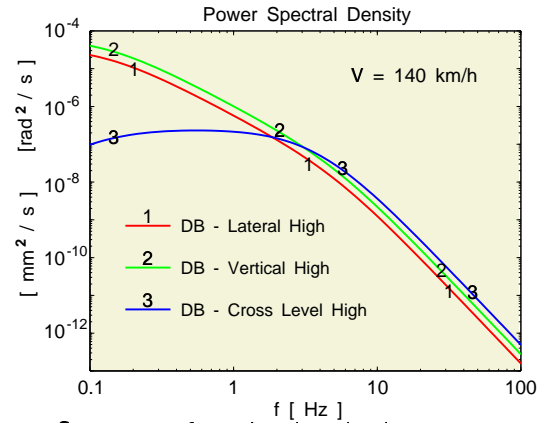


Figure 13. Spectrum of stochastic excitation

Force (see figure 3)	RMS [N]
secondary suspension f_1	1939
f_2	2125
f_3	1950
f_4	2138
primary suspension f_5	2653
f_6	2630
f_7	2733
f_8	2767

Table 1. Riding on straight track: RMS values for dynamical loads in vertical direction

critical location	D/D_{max} for	
	passing switches	ride on straight track
1	0.90	1.00
2	0.48	0.61

Table 2. FATIGUE results

FATIGUE. This enables the calculation of the time history of stresses. The advantage of the way proposed here, is the possibility to perform lifetime calculations without simulating the the whole time of vehicle life. Nevertheless all relevant operational conditions and in particular their frequency can be taken into account. The methodology described in this paper is general. So other lightweight constructions as e.g. aeroplanes or cars also can be investigated with the developed tools FEMBS⁻¹ and FATIGUE.

ACKNOWLEDGMENT

Thanks go to Dipl.-Ing H. Waldeck, Dipl.-Ing R. Gansekow, Dipl.-Ing B. Osterloh and Dipl.-Ing M. Jochim from DUEWAG AG Main Line Rolling Stock Krefeld-Uerdingen for providing realistic FEM and MBS model data. We also would like to thank Dr.-Ing S. Stichel for preparing the basics of the fatigue calculations and inspiring discussions.

REFERENCES

- Braun, B.: *Interface zwischen MKS- und FEM-Programmen zur Spannungsanalyse elastischer Fahrzeugkomponenten*, Fachhochschule München, Fachbereich 04 Elektrotechnik Studienrichtung Datentechnik, Diplomarbeit 1995.
- Dietz, S. and Knothe, K.: *Reduktion der Anzahl der Freiheitsgrade in Finite-Element-Substrukturen*, Bericht aus dem Institut für Luft- und Raumfahrt der Technischen Universität Berlin, Nr 315, 1997.
- Rulka, W.: *SIMPACK - An Analysis and Design Tool for Mechanical Systems*, in *Multibody Computer Codes in Vehicle System Dynamics*, edited by W.Kortüm and R.S.Sharp, Swets & Zeitlinger, pp. 122-126, 1993.
- Stichel, S.: *Betriebsfestigkeitsberechnung bei Schienenfahrzeugen anhand von Simulationsrechnungen*, VDI-Fortschrittsbericht, Reihe 12, Nr. 288, 1996.
- Stribersky, A., Rulka, W., Netter, H. and Haigermoser A.: *Modeling And Simulation of Advanced Rail Vehicles*, Proceedings of the 8th IFAC/IFIP/IFORS Symposium on Transportation Systems '97, Chania, Greece.
- Wallrapp, O. and Sachau, D.: *Space Flight Dynamic Simulations Using Finite Element Analysis Results in Multibody System Codes*, 2nd Int. Conf. on Computational Structures Technology, Athens, Greece, 1994, Civil-Comp-Press.
- Wallrapp, O.: *Standardization of Flexible Body Modelling in Multibody System Codes - Part I: Definition of Standard Input Data*, *Mechanics of Structures and Machines*, 22(3), 1994, pp. 283-304.